2015 IEEE Conference on Control Applications (CCA)
Part of 2015 IEEE Multi-Conference on Systems and Control
September 21-23, 2015. Sydney, Australia

# Reduced LPV Model Development and Control of a Solution Copolymerization Reactor

Sandy Rahme[1], Hossam S. Abbas[2], Nader Meskin[1], Roland Tóth[3] and Javad Mohammadpour[4]

*Abstract*— **In this paper, a linear parameter-varying (LPV) model of a solution copolymerization reactor is developed by taking into consideration the time-varying nature of the parameters in the process. The aim is to design a controller that can ensure the stability and the desired performance of the copolymerization reactor in a prescribed range of operation. The LPV model complexity in terms of the number of scheduling variables is reduced by means of the application of a parameter set mapping (PSM) method which has proven to be effective in reducing the conservatism in LPV model development. The reduced model which only depends on one scheduling variable allows to reduce the complexity of the LPV controller synthesis for the process. Simulation results using the nonlinear model of the copolymerization reactor are provided to illustrate the improvements brought by the LPV controller in terms of reducing the convergence time and the control effort in comparison with a previously developed model predictive controller for the copolymerization process.**

## I. Introduction

The polymer manufacturing is an important field in the chemical industry due to the high consumer demands and the tight market competition for producing different grades of polymers [1]. Therefore, controlling the operation of polymer reactors is a highly important task by aiming at maximizing the production rate and the product quality and also minimizing the transition losses. However, the control design task is nontrivial due to the nonlinear behavior of polymer reactor systems which exhibit strong dependence on multiple operating regimes [2], [3], [4]. Furthermore, the polymer reactors exhibit unstable modes at some operating points [5] as well as time-varying parameters that need to be measured since a polymerization reactor switches through different operating points depending on the needed polymer grades [4]. Moreover, due to the existence of unmeasured disturbances influencing these systems, the development of a robust control strategy is highly desired. Several control approaches have been investigated in the literature [3], [4]. For example, a classical PID controller is developed in [6] without the need of an accurate dynamical model. However, PID controllers are not adequate to cope with such complex systems, in which strong interactions reside between the controlled variables. Hence, model predictive control (MPC) based on simple process models has been proposed in [3] and [7] where a rapid transition between two typical operating points is ensured. A nonlinear controller has been designed and validated experimentally in [2], which depends on online measurements of time-varying model parameters of the nonlinear model of the process.

In order to take the nonlinearity and the time-varying parameters of the process into account, a linear parameter-varying (LPV) $\mathcal{H}_\infty$ control technique (see [8]) is considered in this paper to control a free radical solution copolymerization reactor (see [6]). LPV systems describe a class of nonlinear/time-varying systems that can be represented in terms of parametrized linear dynamics in which the model coefficients depend on a number of measurable variables called scheduling variables [9], [10]. The LPV method provides a powerful tool for designing controllers for nonlinear/time-varying plants [11]. The LPV controller synthesis tools extend the well-known methods of controlling linear time-invariant (LTI) systems to control nonlinear systems and to guarantee stability and high performance over a wide range of operation [12], [13], [14], [15].

The design of LPV controllers often involves two major problems: the presence of many scheduling variables in the system, as is the case in the copolymerization reactor, and the modeling conservatism [16]. For the standard LPV-$\mathcal{H}_\infty$ design approach with polytopic models [8], the number of linear matrix inequalities (LMIs) to be solved increases exponentially with the number of scheduling variables so the control synthesis problem becomes intractable if the dimension of the scheduling variables exceeds three [17]. On the other hand, the range of the scheduling variables often allows the LPV system to include some behaviors that are not exhibited by the real plant due to the dependence of the scheduling variables on the physical variables, which results in conservatism. One way to reduce this conservatism is to *resize* the scheduling regime such that it matches the real system behavior as closely as possible [18]. The parameter set mapping (PSM) procedure based on principal component analysis (PCA) [16] is an effective way to reduce the conservatism in LPV modeling with a reduced number of scheduling variables [19].

In this paper, first an exact LPV representation of the

*This publication was made possible by NPRP grant No. 5-574-2-233 from the Qatar National Research Fund (a member of Qatar Foundation). The statements made herein are solely the responsibility of the authors.

[1]Dept. of Electrical Engineering, College of Engineering, Qatar University, PO Box 2713 Doha, Qatar, sandy.rahme, nader.meskin@qu.edu.qa

[2]Electrical Engineering Dept., Faculty of Engineering, Assiut University, 71515 Assiut, Egypt, hossam.abbas@aun.edu.eg

[3]Control Systems Group, Eindhoven University of Technology, P.O. Box 513, 5600 MB Eindhoven, The Netherlands, r.toth@tue.nl

[4]Complex Systems Control Lab, College of Engineering, The University of Georgia, Athens, GA 30602, USA, javadm@uga.edu

copolymerization reactor is obtained by a transformation procedure capturing the system nonlinearities in the scheduling variables. However, due to the existence of different nonlinear terms in the copolymerization reactor model, the obtained LPV model has 15 scheduling variables. Based on the operating regime of the reactor, the number of scheduling variables is reduced via the PSM method. Then, the $\mathcal{H}_\infty$ LPV control synthesis approach, introduced in [8], is used to synthesize a controller for the reduced LPV model of the reactor. The controller design is done in MATLAB in order to synthesize an LPV controller based on the mixed sensitivity design. In this paper, we intend to emphasize on the capability of the LPV controller, designed on the basis of a reduced model, to provide a high performance control of the polymerization reactor by enhancing the settling time of the output and reducing the control effort.

The paper is organized as follows. In Section II, the nonlinear copolymerization reactor model is introduced. Then, the LPV copolymerization reactor model is presented in Section III. In order to reduce the dimension of the scheduling variables in the LPV model, a parameter set mapping technique is applied in Section IV. The performance of the proposed controller is examined in Section V. Finally, conclusions are drawn in Section VI.

## II. Copolymerization reactor model

Copolymerization is the process of uniting two or more different monomers together to produce a copolymer. In this study, we consider that the monomer A is methyl methacrylate (MMA) and the monomer B is vinyl acetate (VA), the solvent is benzene, the initiator is azobisisobutyronitrile (AIBN), the chain transfer agent is acetaldehyde and the inhibitor is m-dinitrobenzene (m-DNB). These ingredients are continuously added into a well-mixed tank (Fig. 1) where an inhibitor is considered as an impurity and a coolant flows through the reactor jacket to remove the liberated heat via polymerization. The polymer, solvent, unreacted monomers, initiator and chain transfer agent compose the outflow of the reactor. The model of the solution copolymerization reactor

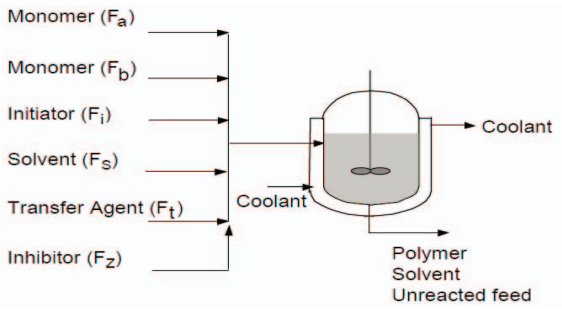


Fig. 1: Copolymerization reactor.

is based on a free radical mechanism [6] described with the differential equations given as follows [3]:

$$
\begin{aligned}
\frac{\mathrm{d}C_k}{\mathrm{d}t} &= \frac{C_{k\mathrm{f}}-C_k}{\theta_\mathrm{r}} - R_k, \quad k=\mathrm{a},\mathrm{b},\mathrm{i},\mathrm{s},\mathrm{t},\mathrm{z},\\
\frac{\mathrm{d}T_\mathrm{r}}{\mathrm{d}t} &= \frac{T_{\mathrm{rf}}-T_\mathrm{r}}{\theta_\mathrm{r}} + \frac{(-\Delta H_{\mathrm{paa}})k_{\mathrm{paa}}C_\mathrm{a}C_\mathrm{a}^{\cdot}+(-\Delta H_{\mathrm{pba}})k_{\mathrm{pba}}C_\mathrm{a}C_\mathrm{b}^{\cdot}}{\rho_\mathrm{r}c_\mathrm{r}}\\
&\quad + \frac{(-\Delta H_{\mathrm{pab}})k_{\mathrm{pab}}C_\mathrm{b}C_\mathrm{a}^{\cdot}+(-\Delta H_{\mathrm{pbb}})k_{\mathrm{pbb}}C_\mathrm{b}C_\mathrm{b}^{\cdot}}{\rho_\mathrm{r}c_\mathrm{r}}\\
&\quad - \frac{U_\mathrm{r}S_\mathrm{r}(T_\mathrm{r}-T_\mathrm{j})}{V_\mathrm{r}\rho_\mathrm{r}c_\mathrm{r}},\\
\frac{\mathrm{d}\lambda_\mathrm{a}}{\mathrm{d}t} &= \frac{-\lambda_\mathrm{a}}{\theta_\mathrm{r}} + R_\mathrm{a},\\
\frac{\mathrm{d}\lambda_\mathrm{b}}{\mathrm{d}t} &= \frac{-\lambda_\mathrm{b}}{\theta_\mathrm{r}} + R_\mathrm{b},\\
\frac{\mathrm{d}\psi_0^\mathrm{p}}{\mathrm{d}t} &= \frac{-\psi_0^\mathrm{p}}{\theta_\mathrm{r}} + \tfrac{1}{2}k_{\mathrm{caa}}(\psi_0^{\mathrm{a}\cdot})^2 + k_{\mathrm{cab}}\psi_0^{\mathrm{a}\cdot}\psi_0^{\mathrm{b}\cdot}\\
&\quad + \tfrac{1}{2}k_{\mathrm{cbb}}(\psi_0^{\mathrm{b}\cdot})^2 + L_1\psi_0^{\mathrm{a}\cdot} + L_2\psi_0^{\mathrm{b}\cdot},\\
\frac{\mathrm{d}\psi_1^\mathrm{p}}{\mathrm{d}t} &= \frac{-\psi_1^\mathrm{p}}{\theta_\mathrm{r}} + k_{\mathrm{caa}}\psi_0^{\mathrm{a}\cdot}\psi_1^{\mathrm{a}\cdot} + k_{\mathrm{cab}}(\psi_0^{\mathrm{a}\cdot}\psi_1^{\mathrm{b}\cdot} + \psi_0^{\mathrm{b}\cdot}\psi_1^{\mathrm{a}\cdot})\\
&\quad + k_{\mathrm{cbb}}\psi_0^{\mathrm{b}\cdot}\psi_1^{\mathrm{b}\cdot} + L_1\psi_1^{\mathrm{a}\cdot} + L_2\psi_1^{\mathrm{b}\cdot},\\
\frac{\mathrm{d}\psi_2^\mathrm{p}}{\mathrm{d}t} &= \frac{-\psi_2^\mathrm{p}}{\theta_\mathrm{r}} + k_{\mathrm{caa}}\left\{(\psi_1^{\mathrm{a}\cdot})^2 + \psi_0^{\mathrm{a}\cdot}\psi_2^{\mathrm{a}\cdot}\right\}\\
&\quad + k_{\mathrm{cab}}(2\psi_1^{\mathrm{a}\cdot}\psi_1^{\mathrm{b}\cdot} + \psi_2^{\mathrm{b}\cdot}\psi_0^{\mathrm{a}\cdot} + \psi_2^{\mathrm{a}\cdot}\psi_0^{\mathrm{b}\cdot})\\
&\quad + k_{\mathrm{cbb}}\left\{(\psi_1^{\mathrm{b}\cdot})^2 + \psi_0^{\mathrm{b}\cdot}\psi_2^{\mathrm{b}\cdot}\right\} + L_1\psi_2^{\mathrm{a}\cdot} + L_2\psi_2^{\mathrm{b}\cdot},
\end{aligned}
\tag{1}
$$

where $C_{k\mathrm{f}} = \frac{F_k}{Q_\mathrm{f}M_k}$, $Q_\mathrm{f} = \frac{\sum_k F_k}{\rho_\mathrm{r}}$, $\theta_\mathrm{r} = \frac{V_\mathrm{r}}{Q_\mathrm{f}}$, $C_k$ is the concentration (kmol/m$^3$), $M$ is the molecular weight (kg/kmol), $Q$ is the volumetric flow rate (m$^3$/s), $R$ is the reaction rate (kmol/m$^3$), $S$ is the surface area (m$^2$), $T$ is the temperature (K), $U$ is the overall heat transfer coefficient (kJ/m$^2$s K), $V$ is the volume (m$^3$), $t$ is the time (s), $\theta$ is the residence time (s), $\lambda$ is the molar concentration of monomer in polymer, $\rho$ is the density (kg/m$^3$), and $\psi_j$ is the $j^{\mathrm{th}}$ moment of molecular weight distribution. The sub and superscripts a, b, i, s, t, z, r, j, p, c are related to monomer A, monomer B, initiator, solvent, chain transfer, inhibitor, reactor, cooling jacket, dead polymer, and combination, respectively, and the superscript (.) represents the free radical. The values of the constant parameters are presented in Table I. For more details on the kinetic and the thermodynamic parameters (such as $k_{\mathrm{paa}}$ and $\Delta H_{\mathrm{paa}}$, respectively), as well as the calculation of the reaction rates $R_k$ $(k=\mathrm{a},\mathrm{b},\mathrm{i},\mathrm{s},\mathrm{t},\mathrm{z})$, the free radical concentrations $C_\mathrm{a}^{\cdot}, C_\mathrm{b}^{\cdot}$, and the moments $\psi^{\mathrm{a}\cdot}, \psi^{\mathrm{b}\cdot}$, the interested reader is referred to [6] (Eqs. (1-12), Eqs. (31-36) and Table 7).

TABLE I: Values for the constant parameters.

| | | | |
|---|---|---|---|
| $M_\mathrm{a}$ | 100.1 (kg/kmol) | $S$ | 4.6 (m$^2$) |
| $M_\mathrm{b}$ | 86.09 (kg/kmol) | $V$ | 1 (m$^3$) |
| $M_\mathrm{i}$ | 164 (kg/kmol) | $U$ | $6.0\times10^{-2}$ (kJ/m$^2$s K) |
| $M_\mathrm{s}$ | 78.11 (kg/kmol) | $c$ | 2.01 (kJ/kg K) |
| $M_\mathrm{t}$ | 44.05 (kg/kmol) | $\rho$ | 879 (kJ/m$^3$) |
| $M_\mathrm{z}$ | 168.11 (kg/kmol) | $T_{\mathrm{rf}}$ | 353.0203 (K) |

TABLE II: Operating conditions.

| | OP1 | OP2 |
|---|---|---|
| $G_{\mathrm{pi}}$ (kg/h) | 23.35 | 24.9 |
| $Y_{\mathrm{ap}}$ | 0.56 | 0.64 |
| $M_{\mathrm{pw}}$ ($10^5$ kg/kmol) | 0.35 | 0.39 |
| $T_\mathrm{r}$ (K) | 353.06 | 353.3 |

The inputs of the system in (1) are the reactor flows $F_\mathrm{a}$, $F_\mathrm{b}$, $F_\mathrm{i}$, $F_\mathrm{s}$, $F_\mathrm{t}$, $F_\mathrm{z}$ and the temperature of the reactor jacket $T_\mathrm{j}$. The important reactor output variables for the product quality control are the reactor temperature $T_\mathrm{r}$, the polymer production rate $G_{\mathrm{pi}}$, the mole fraction of monomer A in

the copolymer $Y_{\rm ap}$, and the average molecular weight $M_{\rm pw}$. Their equations are presented as

$$\begin{aligned} G_{\rm pi} &= (R_{\rm a}M_{\rm a} + R_{\rm b}M_{\rm b})V_{\rm r}, \\ Y_{\rm ap} &= \tfrac{\lambda_{\rm a}}{\lambda_{\rm a}+\lambda_{\rm b}}, \\ M_{\rm pw} &= \tfrac{\psi_2^{\rm p}}{\psi_1^{\rm p}}. \end{aligned} \tag{2}$$

The control objective in this paper is to ensure a fast transition between two steady state operating points given in Table II while rejecting unmeasured disturbance represented by $F_{\rm z}$. It has been shown in [7] that controlling the temperature $T_{\rm r}$ using a PI controller with the manipulated variable $T_{\rm j}$ yields a well-conditioned system and safer conditions. Consequently, the dynamics of $T_{\rm r}$ can be eliminated from the system (1), which reduces the number of states to 11.

## III. Linear parameter-varying modeling

In this section, we develop an LPV representation of the nonlinear model of the copolymerization reactor such that all the system nonlinearities are captured by the scheduling variables. While other methods in LPV modeling, like the Jacobian approach or the state transformation, tend to describe only certain aspects of the original nonlinear behavior, the direct transformation methods generate LPV models that can completely embed in their solution sets the behavior of the original nonlinear model [19]. In continuous time, the state-space representation of an LPV system with static dependency is described as

$$\begin{cases} \dot{x}(t) = A(\theta(t))x(t) + B(\theta(t))u(t), \\ y(t) = C(\theta(t))x(t) + D(\theta(t))u(t), \end{cases} \tag{3}$$

with the state vector $x(t) \in \mathbb{R}^n$, the input vector $u(t) \in \mathbb{R}^m$, the output vector $y(t) \in \mathbb{R}^p$ and the system matrices $A, B, C$ and $D$ are being continuous matrix functions of the scheduling variable vector $\theta(t) \in \mathbb{R}^l$. $\theta(t)$ depends on a vector of measurable signals $\rho(t) \in \mathbb{R}^k$, according to $\theta(t) = q(\rho(t))$, where $q$ is a bounded function. The variable $\theta(t)$ is defined over a compact scheduling set $P_\theta \subset \mathbb{R}^l$ such that $\theta(t) : \mathbb{R}^l \to \mathbb{P}_\theta$. $P_\theta$ is often considered as a polytope and defined as the convex hull given by the vertices $\theta_{{\rm v}_i}$ such that $P_\theta := {\rm Co}\{\theta_{{\rm v}_1}, \theta_{{\rm v}_2}, ..., \theta_{{\rm v}_{\rm L}}\}$, where $L = 2^l$ based on the bounds of $\theta_i$. The LPV representation (3) is called affine in scheduling dependence if the state-space matrices depend affinely on $\theta$ as

$$M(\theta) = M_0 + \sum_{i=1}^{l} \theta_i M_i, \tag{4}$$

where $\theta_i$ is the $i^{\rm th}$ element of $\theta$. Since $\theta$ can be expressed as a convex combination of $L$ vertices $\theta_{{\rm v}_i}$, the system can be represented by a linear combination of LTI models at the vertices. The resulting LPV representation is thus called polytopic where each matrix is represented as

$$Q(\theta) = \sum_{i=1}^{L} \alpha_i Q(\theta_{{\rm v}_i}), \tag{5}$$

such that $\sum_{i=1}^{L} \alpha_i = 1$ with $\alpha_i \geq 0$.

### A. LPV model of the copolymerization reactor

Eliminating the dynamics of $T_{\rm r}$ from (1) results in a nonlinear model with the state vector $x = [C_{\rm a}\, C_{\rm b}\, C_{\rm i}\, C_{\rm s}\, C_{\rm t}\, C_{\rm z}\, \lambda_{\rm a}\, \lambda_{\rm b}\, \psi_0^{\rm p}\, \psi_1^{\rm p}\, \psi_2^{\rm p}]^{\rm T}$, the input vector $u = [F_{\rm a}\, F_{\rm b}\, F_{\rm i}\, F_{\rm s}\, F_{\rm t}\, F_{\rm z}]^{\rm T}$ and the output vector $y = [G_{\rm pi}\, Y_{\rm ap}\, M_{\rm pw}]^{\rm T}$. The equations in (1) nonlinearly depend on the input and the state vectors that are used to construct the signal $\rho(t)$. The nonlinear model (1) can be represented in the LPV form (3) with the state-space matrices shown in (6), where the scheduling variable $\theta(t) \in \mathbb{R}^{15}$ is defined in the Appendix as a vector of complicated functions that depend on $\rho(t)$. For a polytopic LPV model, the number of the LMIs to be solved for the standard $H_\infty$ controller synthesis grows exponentially with the number of scheduling variables according to $M = 2^{l+1} + 1$. With the derived LPV model (3) with $l = 15$, one needs to solve $M = 65537$ LMIs, which is computationally challenging. Therefore, we propose to reduce the number of scheduling variables by applying the parameter set mapping (PSM) method of [16], which is based on Principal Component Analysis (PCA) [19]. An LPV model of the copolymerization reactor can be derived with fewer variables while preserving an acceptable accuracy of representing the original nonlinear model (1).

## IV. Parameter set mapping

The PSM technique can allow to develop an approximate LPV model of the original LPV model with a fewer number of scheduling variables. For LPV models with affine dependence on the scheduling variables, PSM exploits the correlation of the variables and neglects the "less significant" directions in the mapped space. Hence, it allows to obtain lower dimension and tighter range of the scheduling variables and possibly reduce the conservatism. The proposed method also corresponds to a trade-off between the number of scheduling variables and the desired accuracy of the model [16], [19].

### A. Problem formulation and the PSM algorithm

Given the LPV model (3), the problem is to find a mapping $\phi(t) = h(q(t)),\ h : \mathbb{R}^k \to \mathbb{R}^m$, where $m < l$, such that an approximation of the LPV model (3) is obtained as

$$\begin{cases} \dot{x}(t) = \hat{A}(\phi(t))x(t) + \hat{B}(\phi(t))u(t), \\ y(t) = \hat{C}(\phi(t))x(t) + \hat{D}(\phi(t))u(t). \end{cases} \tag{7}$$

The PSM procedure involves the following steps [16], [19]:

1. The first step is to obtain typical trajectories of the scheduling variables, from either measurement or simulation, that cover the expected range of the system operation. These trajectories are collected in a matrix $\Theta \in \mathbb{R}^{l \times N}$ by sampling the scheduling variables at time instants $t = kT,\ (k = 0, 1, ..., N-1)$ with $N \gg l$, or by determining steady-state values of the scheduling variables related to the gridded input space.

2. In order to weight the elements of $\Theta$ equally, a

$$A=\begin{bmatrix}-\theta_1-\theta_2 & 0 & 0 & 0 & 0 & 0 & 0 & 0 & 0 & 0 & 0\\ 0 & -\theta_1-\theta_3 & 0 & 0 & 0 & 0 & 0 & 0 & 0 & 0 & 0\\ 0 & 0 & -\theta_1-\theta_4 & 0 & 0 & 0 & 0 & 0 & 0 & 0 & 0\\ 0 & 0 & 0 & -\theta_1-\theta_5 & 0 & 0 & 0 & 0 & 0 & 0 & 0\\ 0 & 0 & 0 & 0 & -\theta_1-\theta_6 & 0 & 0 & 0 & 0 & 0 & 0\\ 0 & 0 & 0 & 0 & 0 & -\theta_1-\theta_7 & 0 & 0 & 0 & 0 & 0\\ \theta_2 & 0 & 0 & 0 & 0 & 0 & -\theta_1 & 0 & 0 & 0 & 0\\ 0 & \theta_3 & 0 & 0 & 0 & 0 & 0 & -\theta_1 & 0 & 0 & 0\\ \theta_8 & \theta_9 & 0 & 0 & 0 & 0 & 0 & 0 & -\theta_1 & 0 & 0\\ \theta_{10} & \theta_{11} & 0 & 0 & 0 & 0 & 0 & 0 & 0 & -\theta_1 & 0\\ \theta_{12} & \theta_{13} & 0 & 0 & 0 & 0 & 0 & 0 & 0 & 0 & -\theta_1\end{bmatrix}, B=\begin{bmatrix}\frac{1}{M_\mathrm{a}V_\mathrm{r}} & 0 & 0 & 0 & 0 & 0\\ 0 & \frac{1}{M_\mathrm{b}V_\mathrm{r}} & 0 & 0 & 0 & 0\\ 0 & 0 & \frac{1}{M_\mathrm{i}V_\mathrm{r}} & 0 & 0 & 0\\ 0 & 0 & 0 & \frac{1}{M_\mathrm{s}V_\mathrm{r}} & 0 & 0\\ 0 & 0 & 0 & 0 & \frac{1}{M_\mathrm{t}V_\mathrm{r}} & 0\\ 0 & 0 & 0 & 0 & 0 & \frac{1}{M_zV_\mathrm{r}}\\ 0 & 0 & 0 & 0 & 0 & 0\\ 0 & 0 & 0 & 0 & 0 & 0\\ 0 & 0 & 0 & 0 & 0 & 0\\ 0 & 0 & 0 & 0 & 0 & 0\\ 0 & 0 & 0 & 0 & 0 & 0\end{bmatrix},$$

$$C=\begin{bmatrix}0 & 0 & 0000\ 0\ 000\theta_{14}\\ 0 & 0 & 0000\theta_{15}000\ 0\\ M_\mathrm{a}V_\mathrm{r}\theta_2 & M_\mathrm{b}V_\mathrm{r}\theta_3 & 0000\ 0\ 000\ 0\end{bmatrix} \text{ and } D=\mathbb{O}_{3\times 6}. \tag{6}$$

normalization is required. The rows $\Theta_i$ of the data matrix $\Theta$ are normalized such that

$$\Theta_i^\mathrm{n}=\mathcal{N}_i(\Theta_i), \quad \text{with} \quad \bar{\Theta}_i^\mathrm{n}=0, \quad \sigma_i^\mathrm{n}=\sqrt{\mathrm{Var}\{\Theta_i^\mathrm{n}\}}=1,$$

where $\mathcal{N}$ denotes the normalization operator, $\bar{\Theta}_i^\mathrm{n}$ is the sample mean value of $\Theta_i^\mathrm{n}$ and $\sigma_i^\mathrm{n}$ is the sample standard deviation of $\Theta_i^\mathrm{n}$. The normalized data matrix $\Theta^\mathrm{n}\in\mathbb{R}^{l\times N}$ is given by:

$$\Theta^\mathrm{n}=\mathcal{N}(\Theta). \tag{8}$$

3. The PCA method is then applied to the normalized matrix $\Theta^\mathrm{n}$ in (8) in order to find a mapped parameter set with significantly fewer values while retaining most of the information contained in the data. Singular Value Decomposition (SVD) is used to deduce an orthogonal set of basis vectors to $\Theta^\mathrm{n}$ such that

$$\hat{\Theta}^\mathrm{n}=U_\mathrm{s}\Sigma_\mathrm{s}V_\mathrm{s}^\mathrm{T}=U_\mathrm{s}\Phi, \tag{9}$$

where the first $m$ significant singular values are selected in $\Sigma_\mathrm{s}$, and the matrix $U_\mathrm{s}\in\mathbb{R}^{l\times m}$ represents the basis of the significant column space of $\Theta^\mathrm{n}$.

4. The key idea of using PSM as proposed in [19] is to apply the normalized mapping $U_\mathrm{s}$ to determine a parameter function that defines the reduced LPV representation. More specifically, the reduced scheduling variable $\phi(t)$ will be defined via

$$\Phi=U_\mathrm{s}^\mathrm{T}\hat{\Theta}^\mathrm{n} \;\Leftrightarrow\; \phi(t)=U_\mathrm{s}^\mathrm{T}\mathcal{N}(\hat{\theta}(t)). \tag{10}$$

Thus, the mappings $\hat{A},\hat{B},\hat{C},\hat{D}$ in (7) are related to the new scheduling variables $\hat{\theta}(t)$ by [19],

$$\begin{bmatrix}\hat{A}(\phi(t))\ \hat{B}(\phi(t))\\ \hat{C}(\phi(t))\ \hat{D}(\phi(t))\end{bmatrix}=\begin{bmatrix}A(\hat{\theta}(t))\ B(\hat{\theta}(t))\\ C(\hat{\theta}(t))\ D(\hat{\theta}(t))\end{bmatrix}, \tag{11}$$

where the vector $\hat{\theta}(t)$ is defined by

$$\hat{\theta}(t)=\mathcal{N}^{-1}\left(U_\mathrm{s}\phi(t)\right), \tag{12}$$

and $\mathcal{N}^{-1}$ denotes the rescaling operator. Each element of $\hat{\theta}(t)$ is determined as $\hat{\theta}_i(t)=\bar{\Theta}_i+\sigma_i\left(U_\mathrm{s}\phi(t)\right)_i$, where $\bar{\Theta}_i$ and $\sigma_i$ represent the mean and the standard deviation of the rows of the data matrix $\Theta$, respectively. Furthermore, since the LPV model (3) is affine in $\theta$ (4), each matrix in (11) is written as $Q(\hat{\theta}(t))=Q_0+\sum_{i=1}^{l}Q_i\,\hat{\theta}_i(t)$, which leads to

$$\begin{aligned}\hat{Q}(\phi(t))&=Q_0+\textstyle\sum_{i=1}^{l}Q_i\,\bar{\Theta}_i+\sum_{i=1}^{l}Q_i\,\sigma_i\left(U_\mathrm{s}\phi(t)\right)_i\\ &=\underbrace{Q_0+\sum_{i=1}^{l}Q_i\,\bar{\Theta}_i}_{\hat{Q}_0}+\textstyle\sum_{j=1}^{m}\underbrace{\sum_{i=1}^{l}Q_i\,\sigma_i\left(U_\mathrm{s}\right)_{i,j}}_{\hat{Q}_j}\phi_j(t)\\ &=\hat{Q}_0+\textstyle\sum_{j=1}^{m}\hat{Q}_j\,\phi_j(t)\end{aligned} \tag{13}$$

where $(U_\mathrm{s})_{i,j}$ represents the $(i,j)^{\mathrm{th}}$ component of the matrix $U_\mathrm{s}$. This proves that the reduced model is also affine in the reduced scheduling variable $\phi(t)$. At any given time, the mapped vector $\phi(t)$ is computed from (10), which is used to generate the new scheduling variable $\hat{\theta}(t)$ from (12) and then implemented in the original LPV model (3). This leads to a reduced but equivalent LPV model which depends on the new scheduling variable $\hat{\theta}(t)$ [19].

### *B. Reduced model for the copolymerization reactor*

In order to determine the matrix $\Theta$ for the copolymerization reactor model (3) that covers the significant operating points, such as those provided in Table II, the input range is defined as

$$\begin{aligned}18\le F_\mathrm{a}\le 22.5\ \mathrm{kg/h},\\ 87\le F_\mathrm{b}\le 93\ \mathrm{kg/h},\\ 1\le F_\mathrm{t}\le 4\ \mathrm{kg/h}.\end{aligned} \tag{14}$$

The matrix $\Theta$ includes steady-state values of the scheduling variables obtained from solving the nonlinear algebraic equation system (1). Therefore, various scenarios of input combinations are taken into consideration after griding the input range in (14). $\Sigma_\mathrm{s}$ from (9) is obtained as

$$\begin{aligned}\Sigma_\mathrm{s}=[&14.23\ \ 12.2\ \ 6.01\ \ 1.36\ \ 0.58\ \ 0.27\ \ 0.08\ \ 0.03\ \ 0.01\\ &5\times10^{-3}\ \ 2\times10^{-3}\ \ 10^{-3}\ \ 6\times10^{-4}\ \ 10^{-5}\ \ 10^{-6}]^\mathrm{T}.\end{aligned} \tag{15}$$

According to the scheduling dimension considered, the matrix $U_s$ is calculated from (9) and then used for the online calculation of $\phi(t)$ in (10) and $\hat{\theta}(t)$ in (12). For the transition from OP1 to OP2 as shown in Table II, the reduced LPV model provided by the PSM method is simulated with various scheduling dimensions $m=1,2,3$, since the first

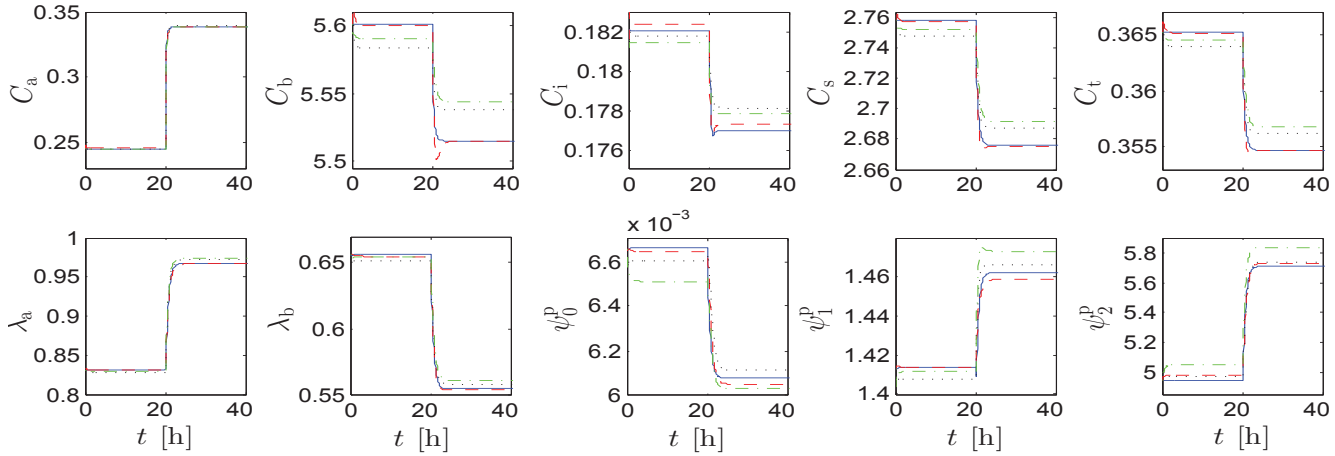


Fig. 2: Simulation based comparison of the state trajectories of the nonlinear model of the copolymerization reactor (solid blue line), PCA-based reduced LPV models: for $m = 1$ (green dash-dotted line), for $m = 2$ (black dotted line) and for $m = 3$ (red dashed line).

three singular values of the matrix $\Sigma_s$ in (15) are the most significant ones. The best fit rate (BFR) of the state evolution between the original state vector $x_{NL}$ and the state vector of the LPV model with reduced scheduling dimension $x_{PSM}$ is calculated as

$$\text{BFR} = 100\% \times \max\left(1 - \frac{||x_{NL} - x_{PSM}||_2}{||x_{NL} - \bar{x}_{NL}||_2}, 0\right), \quad (16)$$

where $\bar{x}_{NL}$ is the sample mean of $x_{NL}$, and $||.||_2$ is the $\ell_2$ norm. The relative accuracy, which represents an indicator of the quality of the reduced LPV model by PSM, is also presented in Table III and derived as the fraction of the total variation $\frac{\sum_{i=1}^{m}\sigma_i^2}{\sum_{i=1}^{15}\sigma_i^2}$, where $\sigma_i$ denotes the $i^{\text{th}}$ singular value of the matrix $\Sigma_s$ in (15). The graphs in Fig. 2 show the states of the original nonlinear model versus the state evolution of the reduced LPV models with scheduling dimensions $m = 1, 2, 3$. In the next section, the reduced LPV models with scheduling dimensions of $m = 1$ and $m = 2$ are considered for synthesizing LPV controllers for the copolymerization reactor.

TABLE III: Accuracy and BFR corresponding to the LPV models with reduced scheduling dimensions.

| | Accuracy (%) | BFR (%) |
|---|---|---|
| $m = 1$ | 55 | 77.8 |
| $m = 2$ | 90.1 | 82.4 |
| $m = 3$ | 99.4 | 96.5 |

## V. Control Design for the Reduced Model

The same control objectives as in [3] are considered for this work and for controlling the reactor temperature $T_r$, a tuned PI controller is taken as in [6] which directly controls the variable $T_j$. It has been demonstrated in [6] that the solution copolymerization reactor is also highly sensitive to changes in the monomer feed ratios and chain transfer agent. Therefore, the manipulated control variables are set to be $F_a$, $F_b$ and $F_t$, and the other inputs are kept constant as $F_i = 0.18$ (kg/h) and $F_s = 36$ (kg/h) [3]. At first, the disturbance caused by an added inhibitor flow is neglected.

The reduced polytopic LPV models of the form (11) with scheduling dimensions of $m = 1$ and $m = 2$ are used to synthesize LPV controllers. The mapped parameter set $\Phi$ obtained from (10) allows defining a set of $2^m$ LTI models on which the LPV-$\mathcal{H}_\infty$ controller has been synthesized by means of the MATLAB Robust Control toolbox command `hinfgs` [8]. The polytopic LPV controller $K(\phi(t))$ defined in (17) is scheduled with respect to the reduced scheduling variable $\phi(t)$ as

$$K(\phi(t)) = \begin{bmatrix} \mathcal{A}_K(\phi(t)) & \mathcal{B}_K(\phi(t)) \\ \mathcal{C}_K(\phi(t)) & \mathcal{D}_K(\phi(t)) \end{bmatrix}. \quad (17)$$

where the matrix functions $\mathcal{A}_K, \mathcal{B}_K, \mathcal{C}_K$ and $\mathcal{D}_K$ are affine in $\phi(t)$. Note that the controller can still receive the information of $T_r$ via the scheduling maps shown in (19) in the Appendix. To meet the control design objectives, the closed-loop is shaped by weighting filter matrices for the sensitivity $W_S$ and the complementary sensitivity $W_K$ channels (Fig. 3) as

$$W_S = \text{diag}\left(\frac{5.352\times10^{-2}}{s+7.49\times10^{-3}}, \frac{4.645\times10^{-6}}{s+6.46\times10^{-6}}, \frac{3.043\times10^{-2}}{s+5.18\times10^{-7}}\right)$$
$$W_K = \text{diag}\left(\frac{7.585s+197}{s+2.597\times10^{4}}, \frac{90.77s+9587}{s+1.056\times10^{5}}, \frac{9.862s+11.37}{s+1153}\right). \quad (18)$$

The sensitivity weighting filter $W_S$ is responsible for tuning the closed-loop bandwidth and ensuring zero steady-state error. The required bandwidth has been inferred from the set of $2^m$ LTI models of the form (11) after freezing the mapped parameter set $\Phi$. On the other hand, the complementary sensitivity weighting filter $W_K$ has been adjusted to impose an upper bound on the control sensitivity in order to restrict the control effort and reduce the output overshoot. The generalized plant is shown in Fig. 3.

An LPV controller, in the form of (17), has been synthesized for each of the reduced LPV models with

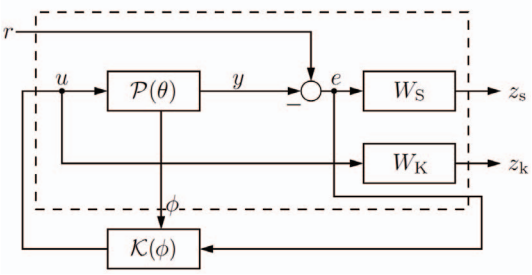


Fig. 3: Generalized plant.

scheduling dimension of $m = 1$ and $m = 2$ and has been simulated with the nonlinear model of the copolymerization reactor (1) in closed loop. The resulting input flow rates and the outputs during the transition from OP1 to OP2 are shown in Figures 4 and 5. Figure 5 shows a fast convergence of the temperature $T_{\mathrm{r}}$ with both $m = 1$ and $m = 2$. The production rate $G_{\mathrm{pi}}$, the polymer composition $Y_{\mathrm{ap}}$ and the molecular weight $M_{\mathrm{pw}}$ take almost 9 hours to converge with $m = 1$ whereas they need 13 hours to reach their steady states with $m = 2$. This result emphasizes the importance of PCA in reducing the model complexity for developing a controller, as well as in providing enhanced closed-loop performance. As discussed in [19], the potential benefit of a tighter set of scheduling variables might not necessarily complicate the controller synthesis and may lead to better closed-loop performance. The LPV-$\mathcal{H}_\infty$ controller provides a higher performance than the MPC controller proposed in [3] whose convergence time is more than 15 hours. Moreover, the input flow rates in Fig. 4 do not reach the saturation levels and the overshoots are less than those shown in [3]. For the inputs $F_{\mathrm{a}}$ and $F_{\mathrm{b}}$, the maximum overshoots in Fig. 4 are $17\%$ and $0.5\%$, respectively, whereas in [3] they reach $50\%$ and $11\%$, respectively. For the other inputs $F_{\mathrm{t}}$ and $T_{\mathrm{j}}$, the overshoots are negligible for the LPV-$\mathcal{H}_\infty$ controller, whereas in [3], the maximum overshoots are $18\%$ and $0.5\%$, respectively. This improvement in the output settling time and the input quality has a significant impact on the industrial process of polymer production.

Finally, the effect of the presence of an inhibitor flow in the reactor feed is studied during the transition from OP1 to OP2, i.e., $F_{\mathrm{z}} \neq 0$, and an inhibitor disturbance of 4 parts per 1000 (mole basis) during the time interval 21.5-23 h is considered as in [3]. The LPV-$\mathcal{H}_\infty$ controller has been designed based on the reduced LPV model with $m = 1$ since this model based control showed the best convergence of the outputs. Unlike the MPC controller developed in [3], Figures 6 and 7 reveal that the LPV-$\mathcal{H}_\infty$ controller rejects the disturbance effect and prevents the saturation and high oscillations of the input flow rates. For the output signals, no oscillations are observed and the convergence interval (around 10 hours) is slower than the case without disturbance, but it remains faster than the response of the controller proposed in [3], which takes more than 15 hours to converge. In addition, in [3], the convergence time of the polymer composition $Y_{\mathrm{ap}}$ is

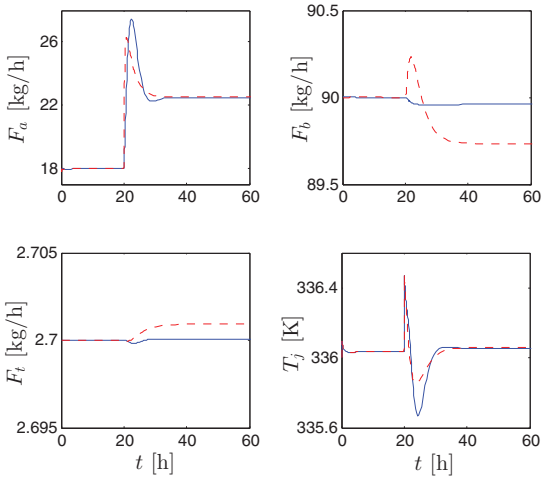


Fig. 4: Control variables during the transition from OP1 to OP2 by the LPV controllers: for $m = 1$ (solid blue line) and for $m = 2$ (red dashed line).

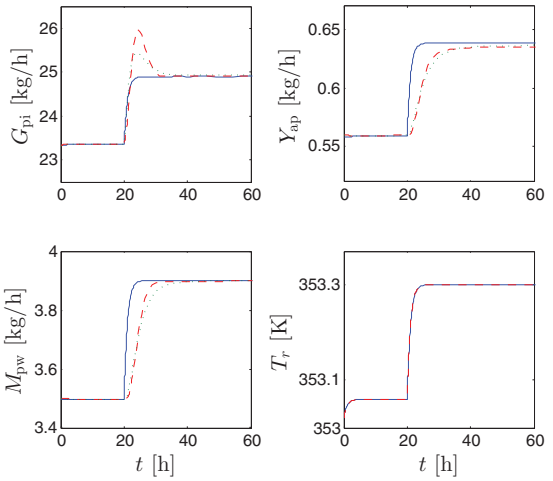


Fig. 5: Output response during the transition from OP1 to OP2 by the LPV controllers: reference (solid blue line), with $m = 1$ (red dashed line) and with $m = 2$ (green dotted line).

longer than 30 hours.

## VI. CONCLUSIONS

In this paper, based on a model transformation approach, an LPV model with a large number of scheduling variables has been developed for the copolymerization reactor. The parameter set mapping based on principal component analysis has been employed to reduce the number of scheduling variables, as well as the conservatism resulting from LPV modeling. Based on the LPV models with reduced scheduling dimensions of 1 and 2, LPV-$\mathcal{H}_\infty$ controllers have been synthesized via the mixed sensitivity-based polytopic approach. The performance of the controllers regulating the original nonlinear model has been successfully demonstrated for a transition between two operating points of the copolymerization reactor. The LPV controller based on scheduling dimension of 1 is shown to provide a better closed-loop

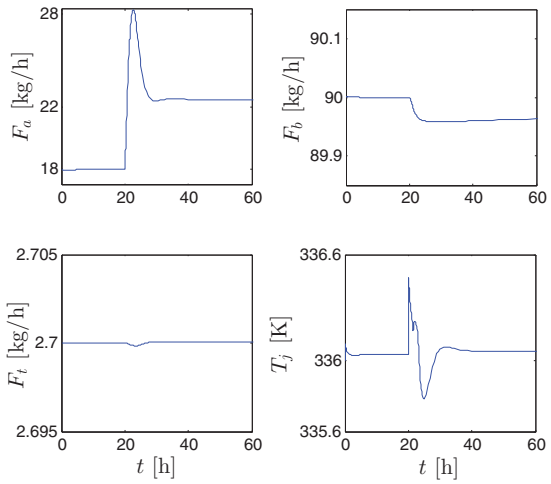


Fig. 6: Control variables during the transition from OP1 to OP2 by the LPV controller in the presence of a disturbance.

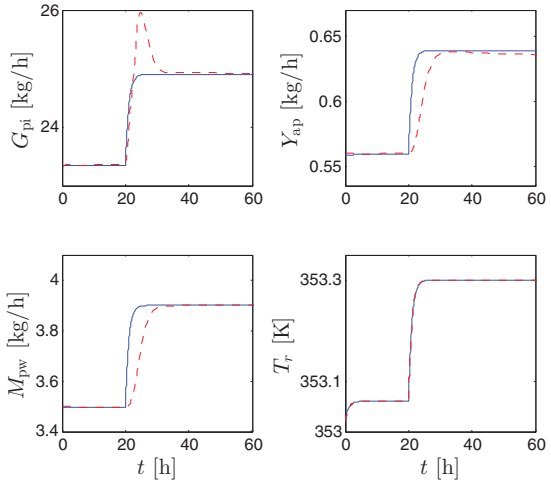


Fig. 7: Output response of the LPV controller during the transition from OP1 to OP2 in the presence of a disturbance (red dashed line) and the reference (solid blue line).

performance due to the low conservatism of the design. Comparing the performance of the synthesized LPV controller with a previously investigated model predictive controller for this application, the LPV controller has shown a better disturbance rejection with no input saturation. The reduced LPV model can be used in future works for developing other LPV control approaches, as well as LPV fault diagnosis of copolymerization reactors.

## VII. APPENDIX

The scheduling variables $\theta_1, \ldots, \theta_{15}$ in the LPV representation of the copolymerization reactor in (3) are defined as

$$
\begin{aligned}
\theta_1 &= \tfrac{1}{\theta_1^{\mathrm{r}}} = f_1(F_{\mathrm{a}}\ F_{\mathrm{b}}\ F_{\mathrm{i}}\ F_{\mathrm{s}}\ F_{\mathrm{t}}\ F_{\mathrm{z}}),\\
\theta_{2-7} &= \tfrac{R_k}{C_k}\ (k = a, b, i, s, t, z) = f_{2-7}(C_{\mathrm{a}}, C_{\mathrm{b}}, C_{\mathrm{i}}, C_{\mathrm{z}}, T_{\mathrm{r}}),\\
\theta_8 &= \tfrac{1}{2}\left(k_{\mathrm{caa}}(\psi_0^{\mathrm{a}\cdot})^2 + k_{\mathrm{cab}}\psi_0^{\mathrm{a}\cdot}\psi_0^{\mathrm{b}\cdot} + L_1\psi_0^{\mathrm{a}\cdot}\right)/C_{\mathrm{a}}\\
&= f_8(C_{\mathrm{a}}, C_{\mathrm{b}}, C_{\mathrm{i}}, C_{\mathrm{s}}, C_{\mathrm{t}}, C_{\mathrm{z}}, T_{\mathrm{r}}),\\
\theta_9 &= \tfrac{1}{2}\left(k_{\mathrm{cbb}}(\psi_0^{\mathrm{b}\cdot})^2 + L_2\psi_0^{\mathrm{b}\cdot}\right)/C_{\mathrm{b}}\\
&= f_9(C_{\mathrm{a}}, C_{\mathrm{b}}, C_{\mathrm{i}}, C_{\mathrm{s}}, C_{\mathrm{t}}, C_{\mathrm{z}}, T_{\mathrm{r}}),\\
\theta_{10} &= \left(k_{\mathrm{caa}}\psi_0^{\mathrm{a}\cdot}\psi_1^{\mathrm{a}\cdot} + k_{\mathrm{cab}}(\psi_0^{\mathrm{b}\cdot}\psi_1^{\mathrm{a}\cdot}) + L_1\psi_1^{\mathrm{a}\cdot}\right)/C_{\mathrm{a}}\\
&= f_{10}(C_{\mathrm{a}}, C_{\mathrm{b}}, C_{\mathrm{i}}, C_{\mathrm{s}}, C_{\mathrm{t}}, C_{\mathrm{z}}, T_{\mathrm{r}}),\\
\theta_{11} &= \left(k_{\mathrm{cab}}(\psi_0^{\mathrm{a}\cdot}\psi_1^{\mathrm{b}\cdot}) + k_{\mathrm{cbb}}\psi_0^{\mathrm{b}\cdot}\psi_1^{\mathrm{b}\cdot} + L_2\psi_1^{\mathrm{b}\cdot}\right)/C_{\mathrm{b}}\\
&= f_{11}(C_{\mathrm{a}}, C_{\mathrm{b}}, C_{\mathrm{i}}, C_{\mathrm{s}}, C_{\mathrm{t}}, C_{\mathrm{z}}, T_{\mathrm{r}}),\\
\theta_{12} &= \left(k_{\mathrm{caa}}\left((\psi_1^{\mathrm{a}\cdot})^2 + \psi_0^{\mathrm{a}\cdot}\psi_2^{\mathrm{a}\cdot}\right) + k_{\mathrm{cab}}(2\psi_1^{\mathrm{a}\cdot}\psi_1^{\mathrm{b}\cdot} + \psi_2^{\mathrm{b}\cdot}\psi_0^{\mathrm{a}\cdot})\right)/C_{\mathrm{a}}\\
&\quad + L_1\psi_2^{\mathrm{a}\cdot}/C_{\mathrm{a}} = f_{12}(C_{\mathrm{a}}, C_{\mathrm{b}}, C_{\mathrm{i}}, C_{\mathrm{s}}, C_{\mathrm{t}}, C_{\mathrm{z}}, T_{\mathrm{r}}),\\
\theta_{13} &= \left(k_{\mathrm{cab}}(\psi_2^{\mathrm{a}\cdot}\psi_0^{\mathrm{b}\cdot}) + k_{\mathrm{cbb}}\left((\psi_1^{\mathrm{b}\cdot})^2 + \psi_0^{\mathrm{b}\cdot}\psi_2^{\mathrm{b}\cdot}\right) + L_2\psi_2^{\mathrm{b}\cdot}\right)/C_{\mathrm{b}}\\
&= f_{13}(C_{\mathrm{a}}, C_{\mathrm{b}}, C_{\mathrm{i}}, C_{\mathrm{s}}, C_{\mathrm{t}}, C_{\mathrm{z}}, T_{\mathrm{r}}),\\
\theta_{14} &= \tfrac{1}{\psi_1^{\mathrm{p}}} = f_{14}(\psi_1^{\mathrm{p}}),\\
\theta_{15} &= \tfrac{1}{(\lambda_{\mathrm{a}}+\lambda_{\mathrm{b}})} = f_{15}(\lambda_{\mathrm{a}}, \lambda_{\mathrm{b}}).
\end{aligned}
\tag{19}
$$

## REFERENCES


[1] M. Embirucu, E. Lima, and J. Pinto, "A survey of advanced control of polymerization reactors," *Polymer Engineering and Science*, vol. 36, no. 4, pp. 433–447, 1996.

[2] M. Soroush and C. Kravaris, "Multivariable nonlinear control of a continuous polymerization reactor: an experimental study," *American Institute of Chemical Engineers Journal (AIChE)*, vol. 39, no. 12, pp. 1920–1937, 1993.

[3] L. Özkan, M. V. Kothare, and C. Georgakis, "Control of a solution copolymerization reactor using multi-model predictive control," *Chemical Engineering Science*, vol. 58, no. 7, pp. 1207–1221, 2003.

[4] J. R. Richards and J. P. Congalidis, "Measurement and control of polymerization reactors," *Computers & chemical engineering*, vol. 30, no. 10, pp. 1447–1463, 2006.

[5] J. P. Congalidis and J. R. Richards, "Process control of polymerization reactors: An industrial perspective," *Polymer Reaction Engineering*, vol. 6, no. 2, pp. 71–111, 1998.

[6] J. Congalidis, J. Richarards, and W. H. Ray, "Feedforward and feedback control of a solution copolymerization reactor," *American Institute of Chemical Engineers (A.I.Ch.E.) Journal*, vol. 35, no. 6, pp. 891–907, 1989.

[7] B. Maner and F. Doyle, "Polymerization reactor control using autoregressive-plus Volterra-based MPC," *American Institute of Chemical Engineers (AIChE) Journal*, vol. 43, no. 7, pp. 1763–1784, 1997.

[8] P. Apkarian, P. Gahinet, and G. Becker, "Self-scheduled $H_\infty$ control of linear parameter-varying systems: a design example," *Automatica*, vol. 31, no. 9, pp. 1251–1261, 1995.

[9] W. J. Rugh and J. S. Shamma, "Research on gain scheduling," *Automatica*, vol. 36, pp. 1401–1425, 2000.

[10] R. Tóth, *Modeling and Identification of Linear Parameter-Varying Systems*. Springer–Verlag, Berlin, Heidelberg, 2010, ch. LPV Systems and Representations.

[11] J. Mohammadpour and C. Scherer, *Control of Linear Parameter Varying Systems with Applications*. Springer-Verlag, New York Dordrecht Heidelberg London, 2012.

[12] Y. Zhao, B. Huang, and J. Chu, "Prediction error method for identification of LPV models," *Journal of Process Control*, vol. 22, no. 1, pp. 180–193, 2012.

[13] R. Tóth, M. Van de Wal, P. Heuberger, and P. Van den Hof, "LPV identification of high performance positioning devices," in *Proc. of the American Control Conference*, San Francisco, CA, USA, 2011, pp. 151–158.

[14] H. S. Abbas, A. Ali, S. M. Hashemi, and H. Werner, "LPV state-feedback control of a control moment gyroscope," *Control Engineering Practice*, vol. 24, no. 3, pp. 129–137, 2014.

[15] A. Bachnas, R. Tóth, J. Ludlage, and A. Mesbah, "A review on data-driven linear parameter-varying modeling approaches: A high-purity distillation column case study," *Journal of Process Control*, vol. 24, no. 4, pp. 272–285, 2014.

[16] A. Kwiatkowski and H. Werner, "Parameter reduction for LPV systems via principle components analysis," in *Proc. 16$^{\mathrm{th}}$ IFAC World Congress*, Prague, Czech Republic, 2005.

[17] C. Hoffmann and H. Werner, "Complexity of implementation and synthesis in linear parameter-varying control," *Proc. of the 19$^{\mathrm{th}}$ IFAC World Congress*, pp. 11 749–11 760, 2014.

[18] T. Azuma, R. Watanabe, K. Uchida, and M. Fujita, "A new LMI approach to analysis of linear systems depending on scheduling parameters in polynomial forms," *Automatisierungstechnik*, vol. 48, no. 4, pp. 119–204, 2000.

[19] A. Kwiatkowski, *LPV Modeling and Application of LPV Controllers to SI Engines*, Ph.D. dissertation, Hamburg University of Technology, Germany, 2008.